

# Slip on faults in the Imperial Valley triggered by the 4 April 2010 Mw 7.2 El Mayor-Cucapah earthquake revealed by InSAR

Meng Wei,<sup>1</sup> David Sandwell,<sup>1</sup> Yuri Fialko,<sup>1</sup> and Roger Bilham<sup>2</sup>

Received 26 August 2010; revised 8 November 2010; accepted 19 November 2010; published 13 January 2011.

[1] Radar interferometry (InSAR), field measurements and creepmeters reveal surface slip on multiple faults in the Imperial Valley triggered by the main shock of the 4 April 2010 El Mayor-Cucapah  $M_w$  7.2 earthquake. Co-seismic offsets occurred on the San Andreas, Superstition Hills, Imperial, Elmore Ranch, Wienert, Coyote Creek, Elsinore, Yuha, and several minor faults near the town of Ocotillo at the northern end of the mainshock rupture. We documented right-lateral slip ( $<40$  mm) on northwest-striking faults and left-lateral slip ( $<40$  mm) on southwest-striking faults. Slip occurred on 15-km- and 20-km-long segments of the San Andreas Fault in the Mecca Hills ( $\leq 50$  mm) and Durmid Hill ( $\leq 10$  mm) respectively, and on 25 km of the Superstition Hills Fault ( $\leq 37$  mm). Field measurements of slip on the Superstition Hills Fault agree with InSAR and creepmeter measurements to within a few millimeters. Dislocation models of the InSAR data from the Superstition Hills Fault confirm that creep in this sequence, as in previous slip events, is confined to shallow depths ( $<3$  km). **Citation:** Wei, M., D. Sandwell, Y. Fialko, and R. Bilham (2011), Slip on faults in the Imperial Valley triggered by the 4 April 2010 Mw 7.2 El Mayor-Cucapah earthquake revealed by InSAR, *Geophys. Res. Lett.*, *38*, L01308, doi:10.1029/2010GL045235.

## 1. Introduction

[2] Surface slip triggered by nearby earthquakes is common on faults in the Salton Trough region of Southern California [Rymer *et al.*, 2002], a regional pull-apart basin formed at a releasing step over between major right-lateral faults associated with the Pacific and the North American plate boundary (Figure 1) [Elders *et al.*, 1972]. The “trough” is filled with sediments mainly from the Colorado River and surrounded by Mesozoic basement rocks and Tertiary volcanic rocks [Dorsey, 2010]. Previous studies have documented triggered slip on faults in the Imperial Valley during more than 8 earthquakes in the last 50 years [Hudnut *et al.*, 1989; Rymer *et al.*, 2002]. Between earthquakes steady surface creep on these faults occurs at rates of a few mm/yr, interrupted by episodic creep events [Rymer *et al.*, 2002; Wei *et al.*, 2009]. Sieh and Williams [1990] infer an association between shallow creep in unconsolidated sediments with inferred high pore pressures. Marone *et al.* [1991] and Du *et al.* [2003] provide a theoretical basis for both steady creep and episodic creep events along the respective faults. They show that in response to steady loading, a velocity-

strengthening zone in the uppermost 3 km can host creep events, whose occurrence time may be advanced by shaking during the passage of seismic waves.

[3] In this study we document triggered slip on faults in the Imperial Valley associated with the 4 April 2010 El Mayor-Cucapah Mw 7.2 earthquake using radar interferometry (InSAR) imagery, field surveys, and creepmeter data. Co-seismic offsets occurred on more than ten faults in this area. We estimate the depth of the triggered slip on the Superstition Hills Fault using dislocation modeling. We find that the results are consistent with previous inferences that slip extends only through the uppermost few kilometers roughly corresponding to the basement depth (3–5 km) [Wei *et al.*, 2009]. The study illustrates that InSAR is an effective tool for measuring small fault offsets. Finally, we discuss the implications for the long-term slip budget. Comprehensive accounts of triggered slip are potentially important for slip budget analysis in the Imperial Valley region as well as seismic hazard assessment.

## 2. Data and Methods

[4] We processed ENVISAT and ALOS InSAR data to study the spatial distribution of slip triggered by the main shock of the 2010 El Mayor-Cucapah earthquake. All InSAR data were processed using GMTSAR, a newly developed software package utilizing Generic Mapping Tools (GMT). The Shuttle Radar Topography Mission (SRTM) Digital Elevation Model [Farr *et al.*, 2007] was used to remove the topographic phase. The best measurements of triggered slip were obtained with 5.6 cm wavelength C-band ENVISAT data, which we found to be less noisy and yielding larger backscatter than the 23.6 cm wavelength L-band ALOS data, especially in the dry lakebed areas such as near the Superstition Hills Fault area. ALOS data were used where either ascending or descending ENVISAT data were unavailable. To maintain the best spatial resolution, all post-processing was done in the radar coordinates using minimal filtering (Gaussian filter with 0.5 gain at 100 m wavelength). Along each fault where we identified triggered slip from the InSAR data, we extracted phase profiles in several locations of the largest offsets. Each of these profiles is 400 meters wide and 4 km long. We estimated the offset as the difference between the maximum and minimum value in the best fitting curve within 200 m of the fault.

[5] In addition to InSAR observations, we measured offsets in the field on the Superstition Hills Fault (SHF), the San Andreas Fault (SAF) and the Imperial Fault (IF). Abrupt triggered slip with negligible afterslip was recorded by creepmeters on the SHF (23 mm) and the southern SAF ( $\approx 5$  mm). In these creepmeter data, the slip occurred between two 5-minute samples and was complete by the

<sup>1</sup>Scripps Institution of Oceanography, La Jolla, California, USA.

<sup>2</sup>CIRES and Department of Geological Sciences, University of Colorado at Boulder, Boulder, Colorado, USA.

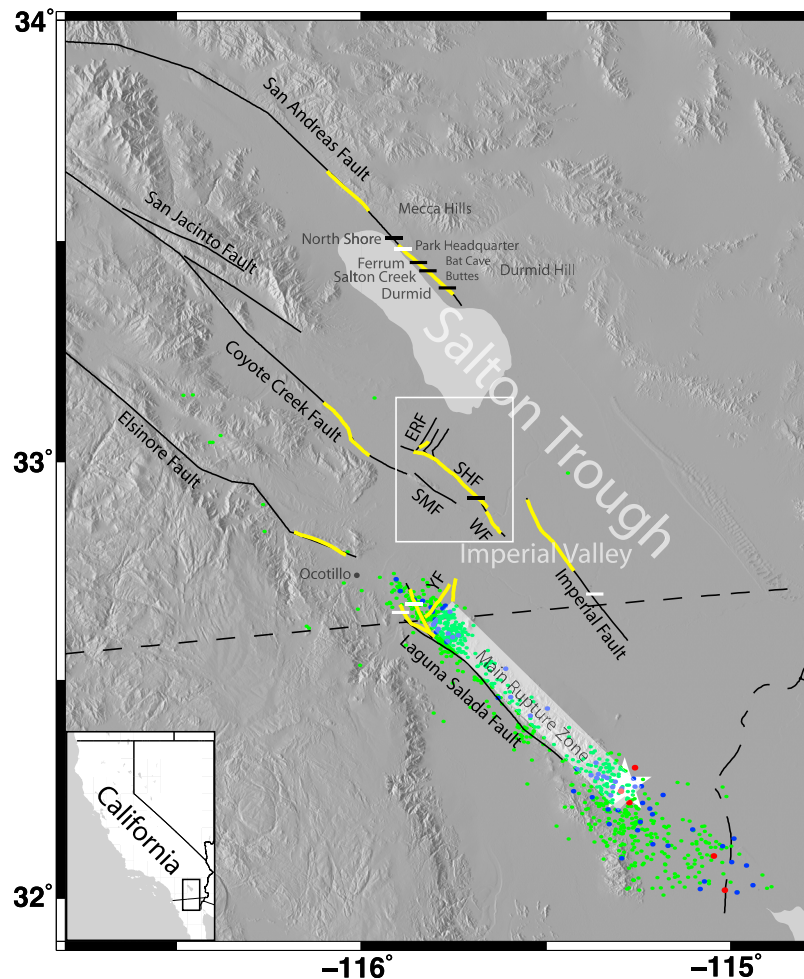


**Figure 1.** Map of Southern California and Northern Baja California. Black solid lines are major faults. Yellow solid lines are faults with observed offsets. Dashed black lines are National and State borders. Black horizontal bars indicate creepmeters operating before April 2010. White horizontal bars indicate creepmeters installed after the earthquake. White star is the epicenter of the 4 April 2010 El Mayor-Cucapah earthquake. Red dots are aftershocks within one month after the main rupture with magnitude greater than 5, blue 4–5, and green 3–4. Earthquake data are from the Southern California Earthquake Center. The mainshock rupture, as revealed by aftershocks and radar interferometry, occurred on largely unmapped faults east of the Laguna Salada Fault. The gray boxes show the locations of InSAR data in Figure 2. Fault names are abbreviated as follows: ERF, Elmore Ranch fault; SHF, Superstition Hills fault; SMF, Superstition Mountains fault; WF, Wienert fault; YF, Yuha Fault.

next sample. The timing coincided with the passage of the seismic waves. Our field survey of the SHF on 9 April, 5 days after the mainshock, revealed surface offsets along more than 10 km of the fault, approximately coincident with the same areas that experienced surface slip during a spontaneous creep episode in 2006 (Figure 2) [Wei *et al.*, 2009]. We measured offsets up to 37 mm following the method described by Rymer *et al.* [2002] and Wei *et al.* [2009]. On 2 May, 28 days after the mainshock, we conducted a survey of the SAF and IF. Since a portion of the SAF had already been surveyed (M. Rymer, personal communication, 2010), we searched for cracks along an unsurveyed area between the Salton Sea Park Headquarters and Bat Cave Buttes where the interferograms show small phase discontinuities, and where three creepmeters also indicate significant slip ( $\sim 5$  mm). The search for fresh cracks was guided by the high-resolution topographic imagery (0.5 m resolution) of the fault trace from the

B4 LiDAR survey [Bevis *et al.*, 2005]. We also searched for cracks along two segments of the IF, at E. Harris Road (W115.53905, N32.88366) and E. McCabe Road (W115.42576, N32.75197). Fresh cracks showing mostly extensional motion were observed on these paved roads, whereas—mostly right-lateral with minor extensional motion was mainly observed in the dirt on the sides of these roads (see Tables S1 and S2 of the auxiliary material).<sup>1</sup>

### 3. Results

[6] InSAR data, field measurements and creepmeters revealed triggered slip on the San Andreas, Superstition Hills, Imperial, Elmore Ranch, Wienert, Coyote Creek, Elsinore, Yuha faults, and several minor faults near the northern end

<sup>1</sup>Auxiliary materials are available in the HTML. doi:10.1029/2010GL045235.

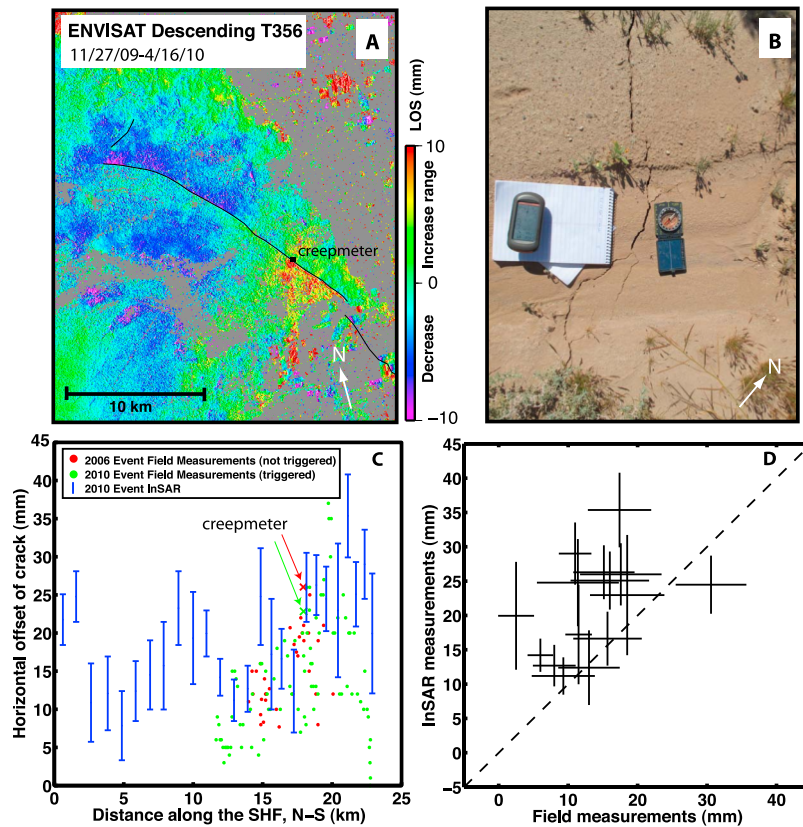


**Figure 2.** (a) InSAR data in radar coordinates show triggered slip on the Superstition Hills Fault and the Elmore Ranch Fault. Solid black lines are the fault traces. White arrow points to North. (b) A photo taken in the field. (c) Slip along the Superstition Hills Fault. (d) Comparison of InSAR measurements with field measurements for the 2010 triggered slip. Dashed line represents the line of ratio 1:1. Solid cross shows the InSAR and Field measurements with uncertainty in segments.

of the Laguna Salada Fault (Figure 1). For all but three of these faults the dominant fault motion is right-lateral strike-slip. The exceptions are sinistral slip on the northeast-striking Elmore and Yuha faults, and a northeast-striking fault about 10 km southeast of the Yuha Fault (Table 1). Because the sense of surface displacements agrees with the long-term fault motion, and the radar phase is essentially discontinuous across the fault trace, we concluded that the observed deformation is due to localized fault slip and not a broad response of compliant fault zones to static stress changes [Fialko, 2004]. Because no significant aftershocks occurred on fault segments that slipped during the time period of our observation (4 April–2 May, 2010), we do not attribute any of the observed slip to aftershocks. Creepmeter data confirm that slip was an abrupt step without significant afterslip.

#### 4. San Andreas Fault

[7] The southern San Andreas Fault is believed to have a high potential for generating a future large earthquake [e.g., Fialko, 2006; Field, 2007]. The seismic moment of such a large earthquake could be reduced by the existence of shallow creep on the SAF triggered by a local or regional event. Triggered slip on this section of the SAF has been observed after numerous nearby earthquakes [Rymer *et al.*, 2002]. Triggered slip associated with the 2010 El Mayor-

Cucapah was observed along 35 km of the southern SAF on the Mecca Hills (15 km) and the Durmid Hill (20 km) segments of the fault as defined by *Bilham and Williams* [1985]. Maximum slip of  $\sim 30$  mm was observed in the Mecca Hills in 2010, where  $\sim 20$  mm of triggered slip also occurred in association with the 1968 Borrego Mountain and 1992 Landers earthquakes [Rymer, 2000]. Comparable slip was also triggered in the Mecca Hills by the 1986 North Palm Springs, the 1987 Superstition Hills [Williams *et al.*, 1988], and the 1999 Hector Mine earthquakes [Rymer *et al.*, 2002]. Fault offsets between North Shore and Salt Creek are discontinuous and poorly expressed. In this area no triggered slip was reported due to the Landers [Rymer, 2000] or Hector Mine earthquakes [Rymer *et al.*, 2002]. Creepmeters at Ferrum, Salt Creek and 1 km south of Bat Cave Buttes (Figure 1) each recorded about 5 mm of slip, and minor surface cracking consistent with 5 mm of slip could be traced  $\pm 1$  km of the southern most creepmeter.

[8] We used ALOS descending data and ENVISAT descending data to distinguish horizontal from vertical triggered offsets on the SAF. ENVISAT ascending data was not used because the Mecca Hills, where the greatest slip occurred is out of the scene coverage (Figure S1). Assuming no fault normal displacement, we estimated  $32.3 \pm 8.1$  mm of horizontal motion and  $8.8 \pm 3.8$  mm of vertical motion (SW side down) on the SAF. The assumption of negligible fault-normal displacement is supported locally at two locations on

**Table 1.** InSAR Derived Slip Amplitude and Direction on Major Faults

Profile ID <sup>a</sup>	Latitude	Longitude	LOS1 (mm) <sup>b</sup>	LOS2 (mm) <sup>b</sup>	Horizontal (mm) <sup>c</sup>	Vertical (mm) <sup>d</sup>
<i>San Andreas Fault</i>						
1	33.603481	-116.018619	12.09 ± 2.04	4.15 ± 0.89	32.3 ± 8.1	-8.8 ± 3.8
2	33.582136	-115.991753	7.37 ± 2.37	2.76 ± 1.46	20.2 ± 10.6	-4.8 ± 5.1
3	33.485131	-115.889969	12.27 ± 3.53	4.87 ± 0.85	30.3 ± 13.3	-6.7 ± 5.5
<i>North Laguna Salada Fault</i>						
4	32.629236	-115.860837	4.80 ± 1.11	7.51 ± 1.33	19.1 ± 2.7	0.6 ± 0.9
5	32.673412	-115.85208	-9.09 ± 2.28	22.96 ± 3.58	41.9 ± 12.9	13.9 ± 2.1
<i>Yuha Fault and an Unknown Northeast Striking Fault</i>						
6	32.680794	-115.790124	21.83 ± 3.01	6.72 ± 1.88	-42.1 ± 5.2	-8.0 ± 1.9
7	32.69424	-115.75064	5.12 ± 1.40	3.35 ± 1.55	-33.4 ± 8.2	-0.8 ± 1.1
<i>Superstition Hills Fault</i>						
8	32.915935	-115.682689	9.15 ± 5.10	8.07 ± 1.40	29.6 ± 4.0	-1.9 ± 1.3
9	32.968969	-115.745803	5.84 ± 1.56	4.71 ± 0.75	18.6 ± 3.1	-1.6 ± 1.0
<i>Elmore Ranch Fault</i>						
10	33.037825	-115.830281	5.54 ± 0.93	0.99 ± 0.62	-9.4 ± 1.6	-2.0 ± 0.6
<i>Coyote Creek Fault</i>						
11	33.030892	-116.002016	1.68 ± 0.98	2.33 ± 0.59	6.9 ± 2.0	-0.2 ± 0.7
12	33.060105	-116.029755	2.03 ± 0.91	1.23 ± 0.87	17.9 ± 6.9	-2.2 ± 1.0
13	33.111056	-116.070245	8.13 ± 1.06	6.03 ± 1.09	26.3 ± 2.8	-3.3 ± 0.9
<i>Elsinore Fault</i>						
14	32.824217	-116.126643	8.35 ± 1.58	2.93 ± 0.65	15.9 ± 2.4	-3.9 ± 1.0

<sup>a</sup>Profile ID number matches the number in Figure S1.

<sup>b</sup>Positive: increase in range direction.

<sup>c</sup>Positive: right-lateral.

<sup>d</sup>Positive: east side up.

Durmid Hill where experimental fault-normal creepmeters had been installed a few months earlier. At both locations fault-normal displacements were <10% of the horizontal slip, an estimate that is limited in accuracy by knowledge of the local strike of the fault.

## 5. Superstition Hills Fault

[9] The SHF has a long history of triggered slip caused by nearby earthquakes in the last several decades [Wei *et al.*, 2009]. For the 2010 earthquake, field measurements and InSAR data show that the entire shallow portion of the Superstition Hills Fault slipped, with a maximum offset of about 37 mm near its southern end. This observation is inconsistent with a model postulating that triggered slip is enhanced at a more distant end of a fault with respect to the seismic source [Fuis, 1982; Rymer *et al.*, 2002]. Slip on the SHF was predominantly right-lateral with minor vertical motion (Table 1). The distribution of offsets along the fault strike is similar to the distribution mapped in 2006 [Wei *et al.*, 2009] (Figure 2c) as well as to the afterslip following the 1987 event. The similarity of slip patterns in 1987, 2006, and 2010 suggests that all slip is in response to the shallow slip deficit produced by the 1987 earthquake.

[10] We extracted twenty-six InSAR profiles from interferograms across the 25-km-triggered segment of the SHF and converted them to horizontal slip using the known radar incidence angles. The field measurements were binned in the same fashion as the InSAR profiles. The mean value and standard deviation of the binned field measurements provide an estimate of the uncertainties in the field data (Figure 2d). The comparison shown in Figure 2d illustrates that the InSAR measurements are on average 50% larger than the

field measurements. This suggests that a fraction of deformation occurs away from the main trace and probably reflects greater slip on the fault in the subsurface. Overall the generally good agreement between InSAR and field measurements validates InSAR as a tool for measuring small fault offsets.

[11] The broad coverage of the flanks of the fault provided by InSAR also allows one to estimate the depth of the triggered slip. A single profile was extracted and interpreted using an anti-plane dislocation model similar to that of Wei *et al.* [2009]. The model shows that creep extends to a depth of only 3–4 km (Figure S2), similar to the results obtained from slip data from the 2006 event [Wei *et al.*, 2009] and indicates that triggered slip is confined to the thick sedimentary cover imaged by seismic studies [Fuis *et al.*, 1984].

## 6. Other Faults

[12] In addition to the SAF and SHF, we also quantified triggered slip on the Imperial, Elmore Ranch, Wienert, Coyote Creek, Elsinore, Yuha faults, and three minor faults at the northern end of the Laguna Salada Fault. As with the SAF and SHF, repeated slip occurred on the same sections on the Imperial, Weinert, and Coyote Creek faults (Figure S3). In contrast, this is the first report of triggered slip on the Elmore Ranch Fault (Figures 2a and S1) and the Elsinore Fault (Figure S4). This may only be a consequence of these fault segments being remote and hardly accessible for field studies.

[13] Slip was also observed on several minor faults near the town of Ocotillo (Figure 1) near the northern end of the 2010 surface rupture zone (Figure S1). These minor faults are in an area that shows small offsets in the interferograms.

Two of these minor faults are northwest-striking and likely represent an extension of the Laguna Salada Fault. The two faults slip right-laterally. The one on the west has a horizontal-vertical ratio (HVR) of 33:1 and a maximum horizontal slip of 19.1 mm, whereas the other fault has a significant amount of vertical slip (HVR 3:1) with a maximum horizontal slip of 40 mm. The Yuha Fault and another northeast-striking fault are perpendicular to the Laguna Salada Fault, forming a cross-fault system similar to EF/SHF system. Both northeast-striking faults show left-lateral slip (<40 mm). These two faults were previously unmapped and are not currently included in the USGS or SCEC databases.

## 7. Discussion

[14] Surface afterslip on the SHF in the four years following the 1987  $M_w$  6.2 Superstition Hills earthquake amounted to 90 cm [Bilham and Behr, 1992]. Episodic creep events on the SHF in 2006 [Wei et al., 2009] and the 2010 triggered slip observed in this study can be viewed as on-going afterslip because a surface slip deficit remains from the 130 cm co-seismic slip at depth inferred for the 1987 mainshock [Larsen et al., 1992]. We note also that static stress changes due to the El Mayor-Cucapah rupture increased shear stress on the SHF fault. The recorded creep rate on the SHF in the year preceding the 4 April earthquake (0.95 mm/yr) fell to 0.3 mm/yr in the six months following the earthquake, suggesting a complicated time-dependent behavior of shallow creep.

[15] In addition to the 1987 earthquake, in the past 40 years triggered slip has been documented more than seven times on the Superstition Hills fault each with maximum amplitudes of 20–30 mm [Wei et al., 2009, Figure 5]. The accumulated triggered slip on the SHF over the last 40 years thus exceeds 0.16 m, about 16% of the average coseismic slip (1 m) on the fault [Rymer et al., 2002]. Prior to the 1987 earthquake few slip events were recorded and a Caltech creepmeter recorded negligible creep. We assume that creep and triggered slip will continue to release the remaining surface slip deficit on the fault in the interval before the next major earthquake.

[16] A multi-institution study (M. Rymer et al., manuscript in preparation, 2010) documents triggered slip on more than 30 faults in southern California, most of which are in the Yuha Desert. Slip on these faults was not detected by InSAR methods presumably because slip was below the InSAR detection threshold (less than a few mm).

## 8. Conclusions

[17] Triggered slip occurred on numerous faults in the Imperial Valley due to the 4 April 2010 El Mayor-Cucapah earthquake: the San Andreas Fault, the Superstition Hills Fault, the Imperial Fault, the Elmore Ranch Fault, the Wienert Fault, the Coyote Creek Fault, the Elsinore Fault, the Yuha Fault, and several sub-faults near the Northern end of the Laguna Salada Fault. The northwest-striking faults all show mainly right-lateral slip. The northeast-striking Yuha Fault, an unnamed fault north of the Laguna Salada Fault, and the Elmore Ranch Fault show predominantly left-lateral slip. The consistency between slip determined by InSAR and field measurements with minor exceptions shows that InSAR is a useful tool in measuring centimeter-scale fault

offsets. Also, the slip determined by InSAR is on average 50% larger than the slip determined from field measurements, suggesting a fraction of the deformation is away from the main trace. Dislocation modeling of InSAR data from the Superstition Hills Fault shows that triggered slip on the fault was confined to the uppermost 3 km as in previous documented slip events.

[18] **Acknowledgments.** We thank Michael Rymer and John Caskey for reviewing this paper, and K. Luttrell and D. Kilb for their comments on an early version of the manuscript. We thank X. Tong, J. Means, X. Chen, D. Huang (UCSD), R. Mellors (SDSU) and G. Fisch for their help with the fieldwork. We thank M. Rymer (USGS) and his collaborators for the information about their field results in the same area. This work was supported in part by the NSF Geophysics Program (EAR 0811772), the NASA EarthScope Program (the InSAR and Geodetic Imaging Component NNX09AD12G), and SCEC. The creepmeters were funded by USGS grants G10AC0016 and 07HQAG0026 and NSF Rapid EAR-1039474.

## References

- Bevis, M., et al. (2005), The B4 Project: Scanning the San Andreas and San Jacinto fault zones, *Eos Trans. AGU*, 86(52), Fall Meet. Suppl., Abstract H34B-01.
- Bilham, R., and J. Behr (1992), A two-depth model for aseismic slip on the Superstition Hills Fault, California, *Bull. Seismol. Soc. Am.*, 82, 1223–1235.
- Bilham, R., and P. Williams (1985), Sawtooth segmentation and deformation processes on the southern San Andreas Fault, California, *Geophys. Res. Lett.*, 12, 557–560, doi:10.1029/GL012i009p00557.
- Dorsey, R. (2010), Sedimentation and crustal recycling along an active oblique-rift margin: Salton Trough and northern Gulf of California, *Geology*, 38(5), 443–446, doi:10.1130/G30698.1.
- Du, W., L. R. Sykes, B. E. Shaw, and C. H. Scholz (2003), Triggered aseismic fault slip from nearby earthquakes, static or dynamic effect?, *J. Geophys. Res.*, 108(B2), 2131, doi:10.1029/2002JB002008.
- Elders, W. A., R. W. Rex, T. Meidav, P. T. Robinson, and S. Biehler (1972), Crustal spreading in southern California, *Science*, 178, 15–24, doi:10.1126/science.178.4056.15.
- Farr, T. G., et al. (2007), The Shuttle Radar Topography Mission, *Rev. Geophys.*, 45, RG2004, doi:10.1029/2005RG000183.
- Fialko, Y. (2004), Probing the mechanical properties of seismically active crust with space geodesy: Study of the co-seismic deformation due to the 1992  $M_w$  7.3 Landers (southern California) earthquake, *J. Geophys. Res.*, 109, B03307, doi:10.1029/2003JB002756.
- Fialko, Y. (2006), Interseismic strain accumulation and the earthquake potential on the southern San Andreas Fault system, *Nature*, 441, 968–971, doi:10.1038/nature04797.
- Field, E. H. (2007), A Summary of previous working groups on California earthquake probabilities, *Bull. Seismol. Soc. Am.*, 97(4), 1033–1053, doi:10.1785/0120060048.
- Fuis, G. S. (1982), Displacement on the Superstition Hills fault triggered by the earthquake, in *The Imperial Valley, California, Earthquake of October 15, 1979, U.S. Geol. Surv. Prof. Pap.*, 1254, 145–154.
- Fuis, G. S., W. D. Mooney, J. H. Healy, G. A. McMechan, and W. J. Lutter (1984), A seismic refraction survey of the Imperial Valley region, California, *J. Geophys. Res.*, 89(B2), 1165–1189, doi:10.1029/JB089iB02p01165.
- Hudnut, K., et al. (1989), Surface ruptures on cross-faults in the 24 November 1987 Superstition Hills, California, earthquake sequence, *Bull. Seismol. Soc. Am.*, 79, 282–296.
- Larsen, S., R. Reilinger, H. Neugebauer, and W. Strange (1992), Global Positioning System measurements of deformations associated with the 1987 Superstition Hills earthquake: Evidence for conjugate faulting, *J. Geophys. Res.*, 97(B4), 4885–4902, doi:10.1029/92JB00128.
- Marone, C. J., C. H. Scholz, and R. Bilham (1991), On the mechanics of earthquake afterslip, *J. Geophys. Res.*, 96(B5), 8441–8452, doi:10.1029/91JB00275.
- Rymer, M. J. (2000), Triggered surface slips in the Coachella Valley Area associated with the 1992 Joshua Tree and Landers, California, earthquakes, *Bull. Seismol. Soc. Am.*, 90(4), 832–848, doi:10.1785/0119980130.
- Rymer, M. J., J. Boatwright, L. C. Seekins, J. D. Yule, and J. Liu (2002), Triggered surface slips in the Salton Trough associated with the 1999 Hector Mine, California, earthquake, *Bull. Seismol. Soc. Am.*, 92, 1300–1317, doi:10.1785/0120000935.

Sieh, K. E., and P. W. Williams (1990), Behavior of the southernmost San Andreas fault during the past 300 years, *J. Geophys. Res.*, *95*(B5), 6629–6645, doi:10.1029/JB095iB05p06629.

Wei, M., D. Sandwell, and Y. Fialko (2009), A silent Mw 4.7 slip event of October 2006 on the Superstition Hills fault, southern California, *J. Geophys. Res.*, *114*, B07402, doi:10.1029/2008JB006135.

Williams, P. L., S. F. McGill, K. E. Sieh, C. R. Allen, and J. N. Louie (1988), Triggered slip along the San Andreas fault after the 8 July

1986 North Palm Springs earthquake, *Bull. Seismol. Soc. Am.*, *78*(3), 1112–1122.

---

R. Bilham, CIRES and Department of Geological Sciences, University of Colorado at Boulder, Campus Box 399, 2200 Colorado Ave., Boulder, CO 80309-0399, USA.

Y. Fialko, D. Sandwell, and M. Wei, Scripps Institution of Oceanography, 9500 Gilman Dr., La Jolla, CA 92093-0225, USA. (mwei@ucsd.edu)